

Interdependence of absorber composition and recombination mechanism in Cu(In,Ga)(Se,S)₂ heterojunction solar cells

M. Turcu, O. Pakma,^{a)} and U. Rau^{b)}

Institute of Physical Electronics (IPE), University of Stuttgart, Pfaffenwaldring 47, 70569 Stuttgart, Germany

(Received 13 December 2001; accepted for publication 13 February 2002)

Temperature-dependent current-voltage measurements are used to determine the dominant recombination path in thin-film heterojunction solar cells based on a variety of Cu(In,Ga)(Se,S)₂ alloys. The activation energy of recombination follows the band gap energy of the respective Cu(In,Ga)(Se,S)₂ alloy as long as the films are grown with a Cu-poor final composition. Thus, electronic loss in these devices is dominated by bulk recombination. In contrast, all devices based on absorber alloys with a Cu-rich composition prior to heterojunction formation are dominated by recombination at the heterointerface, with activation energies smaller than the band gap energy of the absorber material. These activation energies are independent from the S/Se ratio but increase with increasing Ga/In ratio. © 2002 American Institute of Physics. [DOI: 10.1063/1.1467621]

The Cu-chalcopyrite semiconductors CuInSe₂, CuGaSe₂, CuInS₂ and their alloys provide absorber materials for the to date most efficient thin-film solar cell technology. Record chalcopyrite solar cells are made from Cu(In_{1-x}Ga_x)Se₂ thin-film absorbers with $x \approx 0.15-0.35$, and band gap energy $E_g \approx 1.1-1.2$ eV.¹ The usage of Cu(In_{1-x}Ga_x)(Se_{1-y}S_y)₂ alloys with higher Ga and/or S content and thus with a wider band gap is desirable when aiming towards high open circuit voltage solar cells. However, solar cells based on those wide-gap Cu-chalcopyrites generally deliver a significantly lower device performance compared to the record devices. The main drawback of those wide-gap chalcopyrite devices is the fact that the open circuit voltage V_{OC} does not increase at the same rate as E_g .² Thus, it appears that the recombination mechanism changes either qualitatively or quantitatively upon alloying CuInSe₂ with high contents of Ga and/or S. It is, however, unclear whether this trend results from lower-grade bulk properties of the wide-gap materials^{3,4} or from the less favorable band offset between the CdS buffer layer and the wide-gap chalcopyrite.²

The band diagram in Fig. 1(a) illustrates the basic situation. The discontinuity $\Delta E_C = E_C^{ch} - E_C^{CdS}$ between the conduction band energy E_C^{ch} of the chalcopyrite and E_C^{CdS} of the CdS is close to zero in the case of the standard low-gap Cu(In_{1-x}Ga_x)Se₂ (Ref. 5) but can become large in the case of wide-gap chalcopyrites.² This is because alloying CuInSe₂ with Ga increases E_g almost exclusively by rising E_C^{ch} on the energy scale and alloying with S rises E_C^{ch} by about half the amount of the change in E_g .^{6,7} The situation in Fig. 1(a) is unfavorable because the interface recombination barrier Φ_b^p between the Fermi energy and the valence band edge of the absorber at the CdS/absorber interface is relatively small and electrons from the CdS can (cross-)recombine with holes

from the absorber. Therefore, a high interface recombination current is considered as an important drawback of wide-gap chalcopyrite solar cells.²

At this point, it is important to mention, that there are also two different ways to grow a chalcopyrite thin film: High-efficiency devices based on low-gap Cu(In,Ga)Se₂ absorbers¹ use an overall *Cu-poor* composition of the final film. In the very surface region of those films, a layer with a Cu-poorer composition and a larger band gap with respect to the bulk material develops naturally^{8,9} as sketched in Fig. 1(b). High-gap materials, especially CuInS₂,¹⁰ are grown with a final *Cu-rich* composition where the excess CuS has to be removed by a KCN etch from the film before further device processing.¹¹ After this etching step, the remaining film has a rather stoichiometric composition and there is no Cu-depleted surface layer. For CuGaSe₂, both the Cu-poor and the Cu-rich growth methods are used.¹² In all Cu-poor

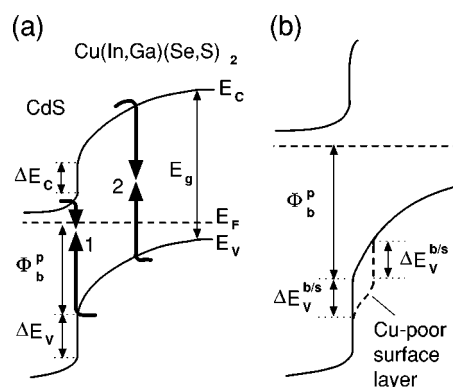


FIG. 1. (a) Band alignments at the interface between CdS and the high-gap Cu(In,Ga)(Se,S)₂ chalcopyrite and possible recombination paths at the heterointerface and in the space charge region of the absorber. The quantities E_C , E_V , E_g , and E_F denote the conduction band, the valence band, the band gap and Fermi energy, respectively, and Φ_b^p indicates the potential barrier for interface recombination. (b) The surface of as-grown Cu-poor chalcopyrite thin films naturally display a Cu-poorer surface layer which widens the band gap of the absorber towards the heterojunction interface by lowering E_V . As a result the barrier Φ_b^p for interface recombination is enlarged.

^{a)}Permanent address: Faculty of Arts and Science, University of Mugla, Turkey.

^{b)}Author to whom all correspondence should be addressed; electronic mail: uwe.rau@ipe.uni-stuttgart.de

Cu(In_{1-x}Ga_x)Se₂-based solar cells, the limiting factor for the open circuit voltage V_{OC} is the recombination in the bulk of the absorber material¹³ while Cu(In,Ga)S₂ (Refs. 14 and 15) and those CuGaSe₂ devices where the films are prepared under Cu-rich conditions¹² are dominated by interface recombination. Therefore, it seems well possible that the borderline between bulk and interface recombination is a matter of Cu-poor and Cu-rich preparation rather than a result of the difference between small-gap and wide-gap materials as argued earlier.²

This letter systematically investigates the composition dependence of recombination in ZnO/CdS/Cu(In,Ga)(Se,S)₂ thin-film solar cells. From temperature-dependent current–voltage measurements (TIV), we find that the activation energy E_a of the recombination follows the band gap energy E_g of the absorber as long as the films are prepared with a final Cu-poor composition. Thus, electronic loss in those devices is dominated by bulk recombination. In contrast, all devices based on absorber alloys with a Cu-rich composition prior to heterojunction formation are dominated by recombination at the heterointerface with an activation energy $E_a < E_g$. Moreover, E_a is independent from the S/(S+Se) ratio y but increases as long as E_g is increased by Ga alloying.

Cu(In_{1-x}Ga_x)(Se_{1-y}S_y)₂ absorber layers are prepared by coevaporation of the elements onto Mo-coated soda lime glass. We use a single-step evaporation procedure with the evaporation rates of all elements kept constant until an approximately 2 μ m thick film is deposited. Due to the geometrical arrangement of the evaporation sources, we obtain samples with overall Cu-poor and Cu-rich composition from the same preparation run. The absorber material is etched in KCN solution prior to heterojunction formation to remove the excess Cu(Se,S) secondary phases¹¹ from the Cu-rich part of the film. Device finalization is accomplished by chemical bath deposition of a 50 nm thick CdS buffer layer and by sputter deposition of a 300 nm thick ZnO window layer followed by the evaporation of an Al metal grid as a front contact. The absorber composition is determined by energy dispersive x-ray spectroscopy. TIV measurements are made using a liquid-N₂ cooled cryostat and a Keithley 2400 source meter. A halogen lamp serves for illuminating the sample and a set of neutral density filters for adjusting the light intensity. For the determination of the absorber band gap energy, we use spectral quantum efficiency measurements.

The evaluation of the TIV measurements uses the short circuit current densities j_{SC} and the open circuit voltages V_{OC} at the various temperatures and illumination intensities. The interdependence of j_{SC} and V_{OC} is given by¹⁶

$$j_{SC} = j_0 \exp\left(\frac{qV_{OC}}{AkT}\right) = j_0 \exp\left(\frac{qV_{OC}}{AkT}\right) \exp\left(\frac{-E_a}{AkT}\right), \quad (1)$$

where A and j_0 are the ideality factor and the saturation current density of the diode, kT/q is the thermal voltage, j_0 is a weakly temperature-dependent prefactor, and E_a is the activation energy of recombination. Resolving Eq. (1) for V_{OC} yields

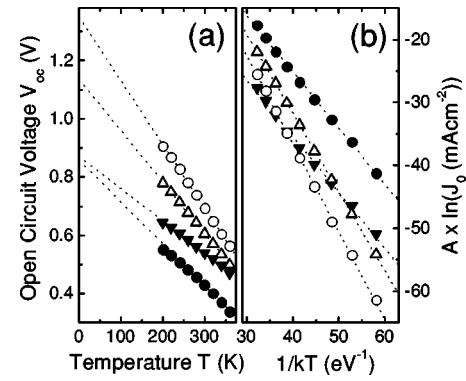


FIG. 2. (a) Extrapolation of the open circuit voltage V_{OC} toward 0 K for Cu-rich (full symbols) and Cu-poor (open symbols) ZnO/CdS/Cu(In_{1-x}Ga_x)(Se_{1-y}S_y)₂ heterojunction solar cells. (b) The corrected saturation current density $A \ln(j_0)$ versus inverse thermal energy $1/kT$ for the corresponding heterojunctions in (a). The slopes provide the activation energies E_a of the recombination process; closed circles: $x=0$, $y=0.41$, $E_g=1.15$ eV, and $E_a=0.90$ eV; closed triangles: $x=0$, $y=0.87$, $E_g=1.43$ eV, and $E_a=0.89$ eV; open triangles: $x=0.25$, $y=0.27$, $E_g=1.22$ eV, and $E_a=1.25$ eV; open circles: $x=0.31$, $y=0.54$, $E_g=1.49$ eV, and $E_a=1.40$ eV.

$$V_{OC} = \frac{E_a}{q} - \frac{AkT}{q} \ln\left(\frac{j_0}{j_{SC}}\right). \quad (2)$$

If A , j_{SC} , and j_0 are independent of temperature T , a plot of V_{OC} versus T should yield a straight line and the extrapolation of this line to $T=0$ K gives the activation energy. Reorganizing Eq. (1) yields the relationship

$$A \ln(j_0) = \frac{-E_a}{kT} + A \ln(j_{00}). \quad (3)$$

Thus, a plot of the corrected saturation current density $A \ln(j_0)$ versus the inverse thermal energy $1/kT$ should yield a straight line where the slope provides E_a . This activation energy is either the band gap energy E_g in case of bulk recombination [path 2 in Fig. 1(a)], or the barrier Φ_b^p in case of interface recombination (path 1).

The extrapolation of V_{OC} to $T=0$ K is illustrated in Fig. 2(a) for several devices made from Cu-rich or Cu-poor Cu(In,Ga)(Se,S)₂ absorbers. The extrapolated values correspond to the band gap energy of the absorbers for the Cu-poor devices, whereas the extrapolation for the Cu-rich devices yields $V_{OC}(0)$ which is considerably smaller than E_g/q . The modified Arrhenius plots of $A \ln(j_0)$ versus $1/kT$ for the same samples as in Fig. 2(a) are shown in Fig. 2(b), where the saturation currents are obtained from the analysis of the illuminated current–voltage characteristics by plotting j_{SC} versus V_{OC} for different illumination intensities. The slopes of the Arrhenius plots yield activation energies which are similar to the extrapolated values $V_{OC}(T=0)$ from Fig. 2(a). Thus both methods yield consistent results.

Figure 3 plots the activation energy E_a obtained from corrected Arrhenius plots of various Cu(In_{1-x}Ga_x)(Se_{1-y}S_y)₂ devices as a function the absorber band gap energy E_g . Let us first discuss the absorbers grown with a Cu-rich final composition. Here, the activation energy of all CuIn(Se_{1-y}S_y)₂ devices is approximately 0.9 V independently from E_g and the Cu-rich Cu(In_{1-x}Ga_x)(Se_{1-y}S_y)₂ devices ($x \approx 0.25$) exhibit E_a of around 1.1 V again independently from E_g . Thus, $E_a < E_g$ holds in all Cu-

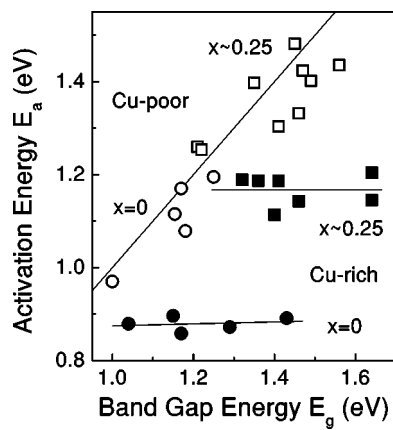


FIG. 3. Activation energies E_a of the recombination process as a function of the band gap energy E_g of Cu-poor (open symbols) and Cu-rich (full symbols) $\text{Cu}(\text{In}_{1-x}\text{Ga}_x)(\text{Se}_{1-y}\text{S}_y)_2$ absorbers with various y and with $x=0$ (circles) and $x\approx 0.25$ (squares). The activation energy for the Cu-poor devices follows the band gap energy of the absorber material. In the case of Cu-rich devices, the activation energy is independent from the band gap energy E_g as long as the variation of E_g is achieved by varying the S/(S+Se) ratio y at a constant Ga/(Ga+In) ratio x .

rich devices which are therefore dominated by interface recombination and the measured E_a corresponds to the potential barrier Φ_b^p [see Fig. 1(a)]. Interestingly, this barrier is not affected by the S/Se ratio, whereas an increase of the Ga/(Ga+In) ratio x increases Φ_b^p by about the same amount as E_g is increased by the Ga admixture. Apparently, the decrease of E_V expected under S/Se alloying^{6,7} is compensated by a decreasing Fermi energy position at the heterointerface, such that the barrier Φ_b^p remains constant. In turn, the increase of Φ_b^p with increasing Ga/(Ga+In) ratio x must result from an upward shift of the Fermi level at the interface because E_V remains constant when alloying CuInSe_2 with Ga.^{6,7}

The activation energies derived from the Cu-poor devices in Fig. 3 follow the band gap energy E_g regardless whether the band gap variation is achieved by alloying with S or Ga. Thus, *all* $\text{Cu}(\text{In,Ga})(\text{Se,S})_2$ devices grown with a final Cu-poor composition are dominated by bulk recombination. The fact is, however, hard to explain for wide-gap chalcopyrites, as $\Phi_b^p = E_g - \Delta E_C$ is much smaller than E_g for large ΔE_C and the interface recombination should prevail under these circumstances. The fundamentally different recombination behavior of Cu-poor chalcopyrite devices com-

pared to their Cu-rich grown counterparts can only be explained when taking into account the surface layer with a higher band gap energy than that of the bulk material. This band gap widening towards the surface is accommodated by a bulk/surface valence band offset $\Delta E_V^{b/s}$, which is around 0.4 eV in case of CuInSe_2 .^{5,8} Figure 1(b) shows that such a band offset directly increases the barrier Φ_b^p to a value $\Phi_b^p + \Delta E_V^{b/s}$ which is now sufficiently large to eliminate interface recombination.^{14,17} Thus, the present results suggest that the enlargement of the band gap energy towards the film surface is an important and operative element in *all* Cu-poor $\text{Cu}(\text{In,Ga})(\text{Se,S})_2$ films.

The authors thank our colleagues at the IPE, M. Balboul, A. Jasenek, Q. Nguyen, K. Orgassa, F. Pfisterer, and H. W. Schock for fruitful discussions as well as J. H. Werner for continuous support. This work was supported by the German Federal Ministry for Education and Research (BMBF) and by the German-Israeli Foundation (GIF).

- ¹M. A. Contreras, B. Egaas, K. Ramanathan, J. Hiltner, A. Swartzlander, F. Hasoon, and R. Noufi, *Prog. Photovoltaics* **7**, 311 (1999).
- ²R. Herberholz, V. Nadenau, U. Rühle, C. Koble, H. W. Schock, and B. Dimmler, *Sol. Energy Mater. Sol. Cells* **49**, 227 (1997).
- ³G. Hanna, A. Jasenek, U. Rau, and H. W. Schock, *Phys. Status Solidi A* **179**, R7 (2000).
- ⁴J. Reiß, J. Malmström, A. Werner, I. Hengel, R. Klenk, and M. C. Lux-Steiner, *Mater. Res. Soc. Symp. Proc.* **668**, H9.4.1 (2001).
- ⁵M. Morkel, L. Weinhardt, B. Lohmüller, C. Heske, E. Umbach, W. Riedl, S. Zweigart, and F. Karg, *Appl. Phys. Lett.* **79**, 4482 (2001).
- ⁶S.-H. Wei and A. Zunger, *J. Appl. Phys.* **78**, 3846 (1995).
- ⁷M. Turcu, I. M. Kötschau, and U. Rau, *Appl. Phys. A: Mater. Sci. Process.* **73**, 769 (2001).
- ⁸D. Schmid, M. Ruckh, F. Grunwald, and H. W. Schock, *J. Appl. Phys.* **73**, 2902 (1993).
- ⁹D. Schmid, M. Ruckh, and H. W. Schock, *Solar Energy Mater. Sol. Cells* **41**, 281 (1996).
- ¹⁰J. Klaer, J. Bruns, R. Henninger, K. Siemer, R. Klenk, K. Ellmer, and D. Bräunig, *Semicond. Sci. Technol.* **13**, 1456 (1998).
- ¹¹T. Walter, A. Content, K. O. Velthaus, and H. W. Schock, *Solar Energy Mater. Sol. Cells* **26**, 357 (1992).
- ¹²V. Nadenau, U. Rau, A. Jasenek, and H. W. Schock, *J. Appl. Phys.* **87**, 584 (2000).
- ¹³U. Rau, M. Schmidt, A. Jasenek, G. Hanna, and H. W. Schock, *Solar Energy Mater. Sol. Cells* **67**, 137 (2001).
- ¹⁴R. Klenk, *Thin Solid Films* **387**, 135 (2001).
- ¹⁵I. Hengel, A. Neisser, R. Klenk, and M. C. Lux-Steiner, *Thin Solid Films* **361**, 458 (2000).
- ¹⁶U. Rau, A. Jasenek, H. W. Schock, F. Engelhardt, and T. Meyer, *Thin Solid Films* **361**, 299 (2000).
- ¹⁷T. Dullweber, G. Hanna, U. Rau, and H. W. Schock, *Solar Energy Mater. Sol. Cells* **67**, 145 (2001).